Translational Oncology
www.transonc.com

Volume 5 Number 3 June 2012 pp. 180–189 180

High-Throughput Molecular Analysis from Leftover of Fine Needle Aspiration Cytology of Mammographically Detected Breast Cancer[1,2]

Laura Annaratone*, Caterina Marchiò*, Tommaso Renzulli†, Isabella Castellano*,‡, Daniela Cantarella†, Claudio Isella†, Luigia Macrì*,‡, Giovanna Mariscotti‡,§, Davide Balmativola*, Elisabetta Cantanna*, Cristina Deambrogio*, Francesca Pietribiasi¶, Riccardo Arisio#, Fernando Schmitt, Enzo Medico† and Anna Sapino*,‡**

*Department of Biomedical Sciences and Human Oncology, University of Turin, Turin, Italy; †Laboratory of Oncogenomics and Department of Oncological Sciences, Institute for Cancer Research and Treatment, University of Turin, Candiolo, Italy; ‡Breast Unit of the Azienda Ospedaliero-Universitaria San Giovanni Battista di Torino, Turin, Italy; §Institute of Diagnostic and Interventional Radiology, University of Turin, Turin, Italy; ¶Department of Pathology, Santa Croce Hospital Asl 5 Moncalieri, Turin, Italy; #Department of Obstetrics and Gynecology, Sant'Anna Hospital, Turin, Italy; **IPATIMUP: Institute of Molecular Pathology and Immunology of the University of Porto and Medical Faculty of Porto University, Porto, Portugal

Abstract

We investigated whether residual material from diagnostic smears of fine needle aspirations (FNAs) of mammographically detected breast lesions can be successfully used to extract RNA for reliable gene expression analysis. Twenty-eight patients underwent FNA of breast lesions under ultrasonographic guidance. After smearing slides for cytology, residual cells were rinsed with TRIzol to recover RNA. RNA yield ranged from 0.78 to 88.40 μg per sample. FNA leftovers from 23 nonpalpable breast cancers were selected for gene expression profiling using oligonucleotide microarrays. Clusters generated by global expression profiles partitioned samples in well-distinguished subgroups that overlapped with clusters obtained using "biologic scores" (cytohistologic variables) and differed from clusters based on "technical scores" (RNA/complementary RNA/microarray quality). Microarray profiling used to measure the grade of differentiation and estrogen receptor and ERBB2/HER2 status reflected the results obtained by histology and immunohistochemistry. Given that proliferative status in the FNA material is not always assessable, we designed and performed on FNA leftover a multiprobe genomic signature for proliferation genes that strongly correlated with the Ki67 index examined on histologic material. These findings show that cells residual to cytologic smears of FNA are suitable for obtaining high-quality RNA for high-throughput analysis even when taken from small nonpalpable breast lesions.

Translational Oncology (2012) 5, 180–189

Address all correspondence to: Anna Sapino, MD, Department of Biomedical Sciences and Human Oncology, Via Santena 7, 10126 Turin, Italy. E-mail: anna.sapino@unito.it; or Enzo Medico, MD, PhD, Institute for Cancer Research and Treatment, Strada Prov. 142, km 3.95, 10060 Candiolo (TO), Italy. E-mail: enzo.medico@ircc.it

[1]This work was supported by Projects of Relevant Scientific National Interest Ministry of University, "Progetto Ricerca Sanitaria Finalizzata DD12/2008" Regione Piemonte, Rete Oncologica del Piemonte e Valle d'Aosta and Associazione Italiana per la Ricerca Sul Cancro (AIRC) (IG 10787) research fund grants to A.S., and AIRC (IG 9127), Ministry of Health and Regione Piemonte to E.M. The funders had no role in study design, data collection and analysis, decision to publish, or preparation of the article. The authors have declared that no competing interests exist.

[2]This article refers to supplementary materials, which are designated by Table W1 and Figures W1 to W3 and are available online at www.transonc.com.

Received 13 December 2011; Revised 18 January 2012; Accepted 19 January 2012

DOI 10.1593/tlo.11343

Introduction

Mammography-based screening programs have dramatically reduced the size of breast cancers at diagnosis. If on one hand histopathologic diagnosis with pTNM staging is essential for management of patients with neoplastic disease, on the other, pathologists are being confronted with increasing demands, from both clinicians and patients, to provide immunophenotypic and gene expression data for planning personalized therapy [1]. The smaller the size of the lesion, the more limited will be the sampling of the specimens. In these terms, small nonpalpable breast cancers may not be suitable for adequate sampling necessary for molecular analysis. A common problem related to the small size of many breast tumors is that, after core needle biopsies are performed (for cancer diagnosis and immunohistochemistry), minimal or no tumoral tissue remains in the surgical specimen that follows. Many of the RNA molecular studies concerning genetic profiles of tumors are done from fresh tumoral tissue extracted from the surgical specimen (once the diagnosis of cancer is established) and sometimes there remains none. In addition, we also need to take into account that the accuracy of molecular tests is utterly dependent on careful preservation of biologic samples before analysis and then on an adequate sampling of fresh tissues. Different studies [2,3] have demonstrated that substantial RNA degradation may occur during the so-called "cold ischemia time" that refers to the time of transfer from the operation room (or removal of blood supply) to the pathology laboratory. Moreover, surgical manipulation may cause changes in gene expression and thus obscure measures of treatment effects or disease prognosis [4]. An alternative can be to obtain RNA for profiling from fine needle aspiration (FNA) cytology and from core needle biopsies (CNB) [5–12]. Nevertheless, most of the studies were designed to perform dedicated FNA for routine cytologic diagnosis and then either single or multiple FNAs dedicated for RNA extraction and microarray analyses [5–8,10,11]. To our knowledge, only one work describes RNA extraction from unused residual cells after conventional diagnostic procedures [13] (Table 1). Alternatively, FNAs were performed on surgically excised specimens or on xenograft [6,9]. Another study describes immediate cryopreservation of FNA cellular material in RNAlater as a good alternative for obtaining later both RNA and cytospin slides after thawing [14].

In the standard protocol followed at our institute for FNA of breast lesions, the aspirated material is immediately smeared onto the slides and then both needle and syringe are discarded although they retain residual cancer cells. Occasionally, the leftover may be harvested after washing the syringe with a fixative and processed for embedding in a paraffin block for later use for immunophenotyping, particularly for the evaluation of hormone receptor, proliferation index by Ki67, and HER2 expression by immunocytochemistry. However, in our experience, the reliability of immunocytochemical results, particularly of Ki67, can be limited by the hypocellularity of the samples. We considered that although the FNA leftover is not of interest to the pathologist for the onsite diagnosis, it may be an important additional source of fresh cell material, suitable for banking and for assessing prognostic and predictive factors in the preoperative setting using molecular tests. This is of particular significance when dealing with small nonpalpable tumors that represent a high rate of screen-detected lesions, where fresh tissue banking for molecular analysis is impossible.

The aim of this study was to validate the possible use of RNA extracted from cells residual to diagnostic smears obtained from FNA of small nonpalpable breast lesions as an adequate and reliable material for gene expression analysis.

Materials and Methods

Sample Collection

The design of the study illustrated in Figure 1 was approved by the institutional review board of the Breast Unit of the Azienda Ospedaliero-Universitaria San Giovanni Battista di Torino and by the ethic institutional review board for "Biobanking and use of human tissue for experimental studies" of the Department of Human Oncology and Biomedical Science of the University of Torino. The cytology leftovers were collected from 28 diagnostic FNA samples performed in the Radiology Department of San Giovanni Battista Hospital, Turin, from June to July 2010 on mammographically detected opacities. Patients were informed of the study protocol and that it would not interfere with diagnosis or treatment decisions.

All FNAs were performed under ultrasound guidance by an experienced breast radiologist using a 22-gauge needle attached to a syringe inserted into a pistol grip holder. The samples were processed using a standard protocol for FNA diagnosis. The aspirated material was smeared onto two slides; the first one was immediately fixed in methanol for 5 minutes and then stained with hematoxylin and eosin. The second slide was air-dried for Giemsa staining. One milliliter of TRIzol (Invitrogen, Carlsbad, CA) solution was then aspirated with the needle, and after rinsing the syringe, the solution containing the residual material was transferred to a vial and stored on ice. At the end of the FNA session, the vials were transported in ice to the cytology laboratory and stored at −80°C for up to 1 month. An experienced cytopathologist was present onsite to assess the adequacy of the FNA and if the hematoxylin and eosin smear was not suitable for diagnostic purposes, the patient underwent a second FNA. A core biopsy was immediately performed after the FNA, in case of discrepancy between the radiologic risk and the cytologic diagnosis.

For each FNA, the cytologic category "C" proposed by the European Guidelines for breast screening pathology [15] was given to classify the smears together with the final diagnosis (Table 2). Because it is possible that no cellular material remains in the syringe after the preparation of diagnostic smears, we compared the amount of RNA with the smear cellularity to evaluate whether this morphologic parameter could be used for the assessment of adequacy of the leftover. Thus, for the study purposes, cellularity was evaluated independently by two pathologists (A.S. and I.C.) at low magnification (4×), and when cells (including cancer, stromal, and inflammatory cells) were present in less than one third, from one third to two thirds, and more than two thirds of the smear, they were classified as having "low," "intermediate," or "high" cellularity, respectively. The prevalence of normal epithelial, cancer, stromal, and inflammatory cells (lymphocytes *vs* granulocytes) was carefully detailed (Table 2). Nuclear grade was given for neoplastic smears using the criteria proposed by Dabbs and Silverman [16]. In low-nuclear-grade cancers, most of the neoplastic nuclei were small and uniform with smooth membranes and showed fine chromatin and no nucleoli; intermediate-grade nuclei were shown to be up to twice the size of those of low nuclear grade, with moderate pleomorphism, and small nucleoli. High-nuclear-grade specimens showed marked pleomorphism and hyperchromatism and macronucleoli. Lesion size was recorded for each case (Table 2).

RNA Extraction

RNA extraction was performed by rinsing the FNA syringe with 1 ml of TRIzol reagent, according to the manufacturers' instructions. RNA

Table 1. Molecular Studies on FNA Cytology.

Reference	Targeting of Lesion	Onsite Evaluation of FNA Adequacy	No. FNA Sampling	Same Sample for Both Cytology and RNA Extraction	FNA Specimen Storing Condition for Molecular Analysis	Type of RNA Analysis
Assersohn et al. [5]	NS	NO	1	Yes (cytospin)	Cell suspension MEM with phenol red and 25 mM HEPES buffer	cDNA microarray
Centeno et al. [6]	FNA of surgical samples	NO	>2	NO	In TRIzol at −80°C	Agilent 2100 Bioanalyzer and cDNA microarray
Lim et al. [7]	Endoscopy, computed tomography, fluoroscopy	NO	NS	NO	In RNAlater at −80°C	cDNA microarray
Pusztai et al. [8]	Palpation	NS	3-4	NO	In RNAlater or snap-frozen and stored at −80°C	Agilent 2100 Bioanalyzer and cDNA microarray
Sotiriou et al. [10]	NS	NO	NS	NO	Cell suspension in normal saline, snap-frozen in liquid nitrogen and stored at −80°C	cDNA microarray
Symmans et al. [11]	NS	NO	4	NO	In RNAlater or snap frozen in plain vial and stored at −80°C	Agilent 2100 Bioanalyzer and cDNA microarray
Uzan et al. [12]	Ultrasound or palpation	YES	1-2	NO	Lysis solution RLT, a guanidine/thiocyanate–containing buffer (Qiagen)	Agilent 2100 Bioanalyzer and real-time PCR
Wong et al. [28]	Palpation	NO	2 (1 on surgical specimen)	YES (liquid cytology)	RNA extraction lysis buffer (Qiagen, Valencia, CA) and quickly frozen to −80°C	Agilent 2100 Bioanalyzer and cDNA microarrays
Ladd et al. [14]	FNA of surgical specimen	NO	1-2	YES	RNAlater or cryopreservation media	Agilent 2100 Bioanalyzer
André et al. [13]	NS	NO	NS	YES	NS	Agilent 2100 Bioanalyzer and Splice-array profiling
Annaratone et al. (current work)	Ultrasound or stereotaxic mammography	YES	1 or 2	YES	In TRIzol at −80°C	Agilent 2100 Bioanalyzer, RT-PCR and cDNA microarrays

NS indicates not specified.

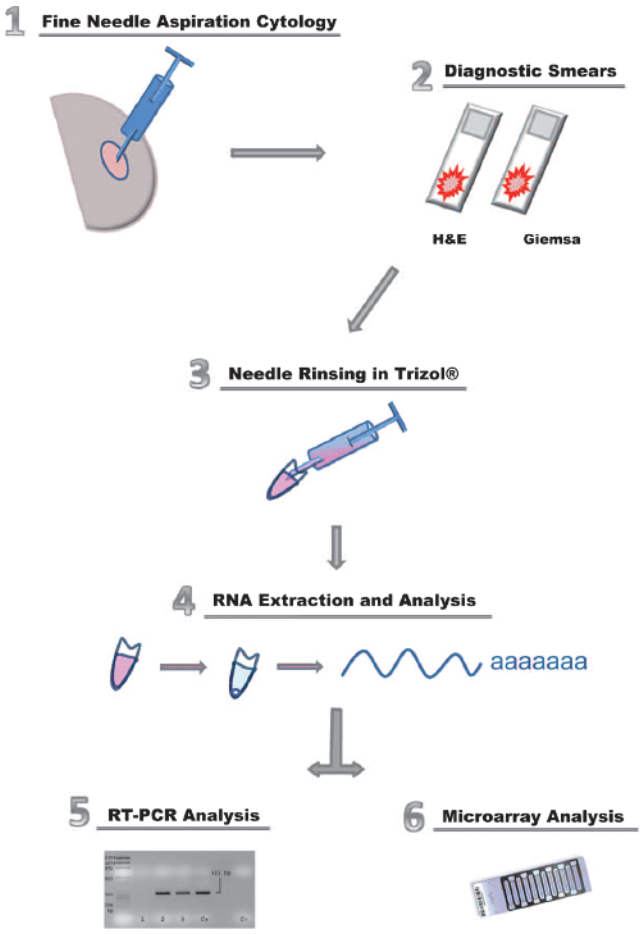

Figure 1. Study flowchart. Flowchart illustrating the design of the study.

pellets were dissolved in a final volume of 35 µl of diethylpyrocarbonate water, left on ice for 1 hour, and then heated to 60°C for 10 minutes.

RNA concentration was assessed using a spectrophotometer (BioPhotomer Eppendorf AG, Hamburg, Germany), and then the distribution of the amount of total RNA (µg) extracted was evaluated. The quality and quantity of the extracted RNA were also assessed using a Bioanalyzer 2100 (Agilent Technologies, Palo Alto, CA) based on a 28S/18S ribosomal RNA ratio and on the "RNA integrity number" (RIN).

Reverse Transcriptase–Polymerase Chain Reaction and Polymerase Chain Reaction Analysis

Reverse transcriptase–polymerase chain reaction (RT-PCR) was performed after a DNAse treatment step with TURBO DNA-free Kit (Ambion, Foster City, CA). For each sample, up to 4 µg of RNA was reverse transcribed to complementary DNA (cDNA) with the High-Capacity cDNA Reverse Transcription Kit (Applied Biosystems, Foster City, CA). RNA samples without reverse transcriptase were reverse transcribed as negative controls of DNA contamination for PCR analyses. Messenger RNA (mRNA) for *PGK* (PGK1, NM_000291.3) was amplified for each sample for quality control of RNA integrity and absence of DNA polymerase inhibitors (forward, 5′-CAgTTTggAgCTCCTggAAg-3′; reverse, 5′-TgCAAATCCA gggTgCAgTg-3′). The *PGK* gene was amplified with a touchdown PCR program [17]. cDNA samples were subsequently amplified for the target sequences by using published primers for *CK19* (KRT19, NM_002276.4) [18]. Each PCR was carried out with a mix containing PCR Buffer 10× (1× final), $MgCl_2$ (2 mM final) POLYTAQ Taq DNA Polymerase (1.5 U final; Polymed, Florence, Italy), dNTPs mix (0.2 mM final), cDNA (200-250 ng), and primers. The reactions were performed on PTC-100 Peltier Thermal Cycler (MJ Research, Inc, Waltham, MA). PCR products were separated by electrophoresis on an agarose gel stained with ethidium bromide. To reduce the risk of contamination from previously amplified products, separate bench areas were used for RNA isolation, amplification, and electrophoresis.

Microarray Data Generation and Analysis

Biotinylated complementary RNA (cRNA) was prepared using the Illumina TotalPrep RNA Amplification Kit (Ambion, Inc, Austin, TX) according to the manufacturer's recommendations starting with 500 ng of total RNA or, when less RNA was available, with lower amounts down to a minimum of 90 ng. Hybridization of the cRNA to the HumanHT-12_V3 Expression BeadChip (Illumina, Inc, San Diego, CA), washing, and scanning were performed according to the Illumina BeadStation 500× manual (revision C). Microarray data were cubic-spline-normalized with the GenomeStudio software (Illumina) and subsequently processed and analyzed using Excel (Microsoft Corp, Redmond, WA). Data were clustered and visualized using the GEDAS software [19]. Bootstrap cluster analysis was performed using the "pvclust" R package [20,21]. Microarray expression data are deposited in Gene Expression Omnibus (GEO accession number GSE22495). Additional details on *in silico* analysis of gene expression and classification of FNA leftover samples are provided in the Supplementary Methods. Statistical power analyses were performed using two online tools: http://www.quantitativeskills.com/sisa/statistics/correl.htm and http://www.dssresearch.com/KnowledgeCenter/toolkitcalculators/statisticalpowercalculators.aspx.

Results

Smear Cellularity, RNA Yield, and RT-PCR Efficiency

As shown in Table 2, total RNA was successfully extracted from all the 28 FNA samples and the mean RNA yield per FNA was 11.7 µg (range, 0.78-88.4 µg; median, 4.85 µg; mode, 7.5 µg).

We then compared the size of the lesions with the amount of RNA yield. The opacities ranged in size from very small and nonpalpable (5 mm, sample 23W) to large palpable lesions (used as control). One case was large enough to be suitable for primary systemic therapy (70 mm, sample 19S). However, even in very small malignant (samples 3C, 4D, and 23W) and in nonmalignant lesions (samples 10J and 28AB), the RNA yield was adequate (Table 2).

Afterward, the cellularity of the smears (classified as high, intermediate, and low) was compared with the amount of RNA extracted from the leftover because it was possible that no cellular material remained in the needle after the preparation of diagnostic smears. As shown in Figure 2*A*, the amount of total RNA (µg) extracted from FNA leftovers correlated well with the amount of cells present on the smear. Regarding the cell type, all the smears displayed a prevalence of epithelial cells (either benign or malignant depending on the nature of the lesion itself), followed by elongated stromal

Table 2. Characteristics of the 28 Samples of FNA Cytology.

No.	Sample	Mammographic Size (mm)	RNA Yield (μg)	Cellularity	Cell Types on Smears			Cytological Category
					Cancer	Stromal	Inflammatory	
1	A	10	1.30	L	80%	20%		C5
2	B	12	4.16	L	70%	30%		C5
3	C	8	5.20	I	60%	35%	5%	C5
4	D	7	7.80	L	100%			C5
5	E	13	8.06	H	80%	15%	5%	C5
6	F	13	9.36	H	100%			C5
7	G	15	10.50	I	60%	30%	10%	C5
8	H	10	11.44	H	90%		10%	C5
9	I	18	12.74	I	90%	10%		C5
10	J	8	2.70	L	*	10%		C3
11	K	10	7.50	I	50%	50%		C5
12	L	13	17.16	I	75%	20%	5%	C5
13	M	14	26.26	H	100%			C5
14	N	12	68.10	H	70%	10%	20%	C5
15	O	11	88.40	H	60%	10%	30%	C5
16	P	10	4.50	I	70%		30%	C5
17	Q	12	5.98	L	75%	5%	20%	C5
18	R	29	7.50	H	70%	5%	25%	C5
19	S	70†	3.30	L	75%	20%	5%	C5
20	T	13	2.10	H	80%	15%	5%	C5
21	U	10	1.80	L	100%			C5
22	V	10	2.08	I	45%	50%	5%	C5
23	W	5	3.64	L	85%	10%	5%	C5
24	X	10	0.78	I	90%		10%	C5
25	Y	15	4.16	H	85%	5%	10%	C5
26	Z	11	3.64	L	100%			C5
27	AA	10	2.60	I	80%	10%	10%	C5
28	AB	7	3.90	L	*			C2

C2 indicates benign; C3, probably benign; C5, malignant; I, intermediate; H, high; L, low.
*One hundred percent of nonneoplastic apocrine cells.
†The patient received neoadjuvant chemotherapy before surgery.

cells or small fragments of connective tissue. Inflammatory cells (lymphocytes or granulocytes) were rare compared with the other cell populations. In five samples, only cancer cells were detected (Table 2).

RNA integrity and absence of DNA polymerase inhibitors were then assessed by the percentage of samples positive for *PGK* housekeeping gene. Of 28 samples, 26 (92.8%) were RT-PCR positive for *PGK* (the negative samples were 1A [lobular breast carcinoma] and 24X [ductal invasive carcinoma with sclerosis]). These 26 samples were tested for *CK19* gene expression, a low-molecular-weight cytokeratin specific for normal and neoplastic breast epithelium. All of them were positive, with the exception of that composed of few apocrine cells (sample 28AB), confirming efficient detection of epithelial cells by PCR (Figure 2*B*).

Analysis of Global Gene Expression Profile

This analysis was performed on 23 of 24 leftover samples classified cytologically as malignant (C5). For these cases, the corresponding histologic specimens were retrieved and reanalyzed for routine prognostic factors (histologic grade, estrogen receptor [ER] expression, progesterone receptor [PgR] expression, proliferation index as determined by Ki67 [%], and HER2 expression). One case was not analyzed because the surgical histologic samples were not available. In addition, lab-on-chip analysis of the FNA leftover with the Bioanalyzer 2100 (Agilent) allowed measuring RNA quality in RIN values (Materials and Methods), which ranged from 4.4 to 8.8 (median, 7.3). RIN values of at least

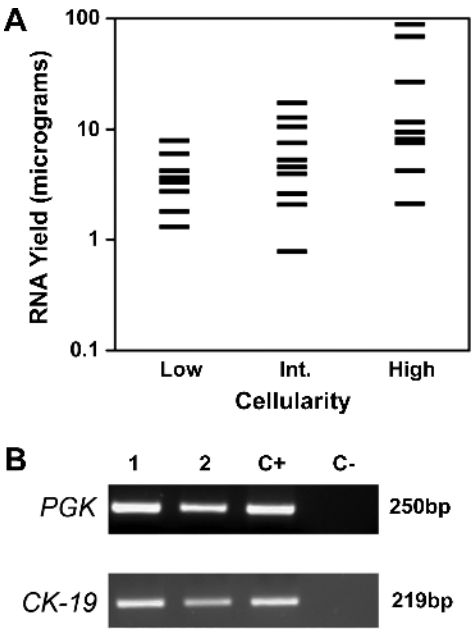

Figure 2. RNA yield and RT-PCR efficiency in FNA leftovers. (A) Distribution of total RNA yield from FNA leftovers. The amount of total RNA micrograms extracted (*y* axis) from FNA leftovers was subdivided in three classes of sample cellularity, namely, high, intermediate, and low, as indicated on the *x* axis. (B) RT-PCR analysis of *PGK* and *CK-19* in FNA leftovers. Lanes 1 and 2, FNA samples. Lane C+, positive control. Lane C−, negative control.

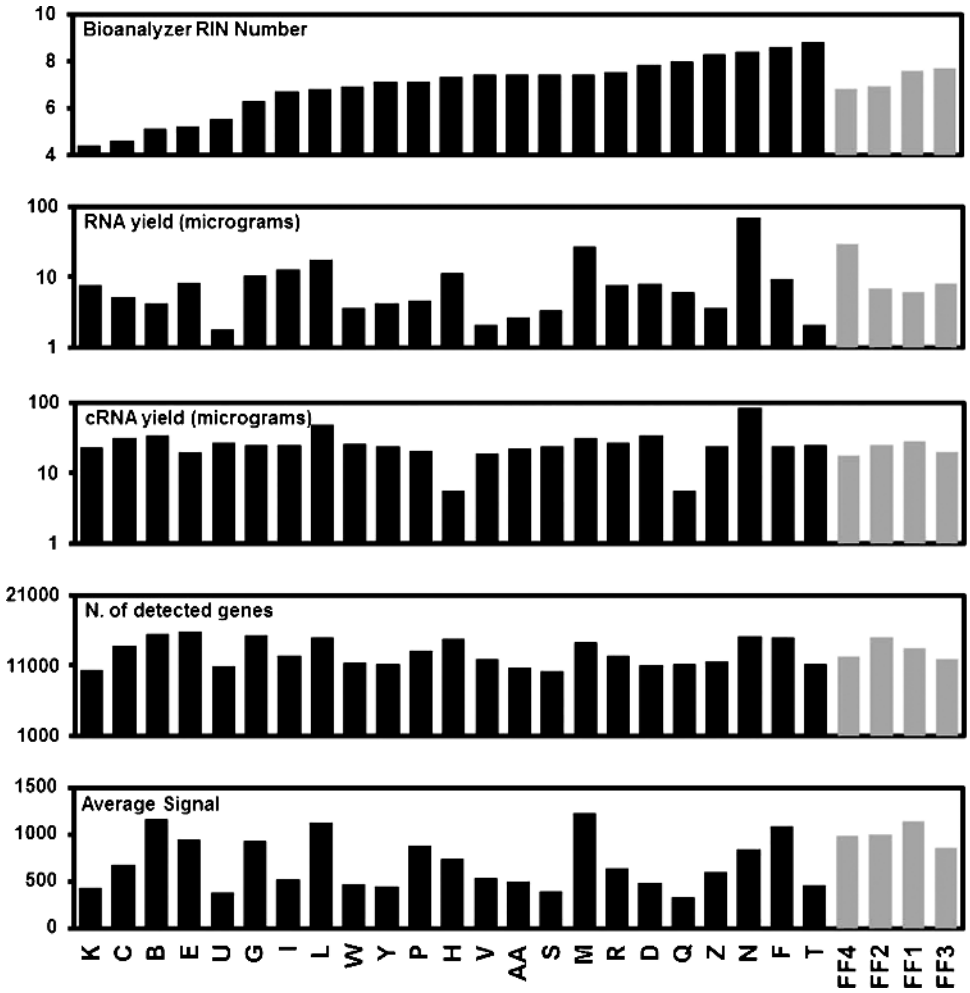

Figure 3. Technical quality controls. For each FNA sample, the following five technical quality control parameters are displayed, from top to bottom as indicated: (top) RIN number measured with the bioanalyzer on the extracted total RNA, RNA yield as measured with the spectrophotometer, cRNA yield as measured with the Bioanalyzer, total number of genes with detection *P* value of 0 after hybridization, and (bottom) average signal on the microarray.

seven are considered adequate for microarray analysis [22]. However, with Illumina arrays, reasonable quality data can be obtained also with samples with lower RIN values (our unpublished observations). Therefore, all the 23 RNA samples were processed for microarray analysis. After reverse transcription and *in vitro* transcription, the amount of cRNA obtained was quantified using spectrophotometer to check that sufficient cRNA was generated also when it was not possible to start from 500 ng of RNA. Finally, we considered two posthybridization microarray quality control parameters: (i) number of detected genes and (ii) average signal; the values obtained from leftovers of FNA were compared to those previously obtained on fully intact RNA from four breast cancer fresh-frozen samples [23]. All the above-mentioned quality control parameters were plotted together to assess possible relationships, as illustrated in Figure 3. No major differences were observed in any parameter between FNA leftovers and fresh-frozen sample. Notably, the RIN number showed no correlation with any other technical parameter: even samples with low RIN values yielded good amounts of cRNA, high numbers of detected genes, and a strong signal. As expected, a high correlation was observed between the number of detected genes and the average signal (Pearson = 0.89) and also between the initial RNA yield and the cRNA yield (Pearson = 0.81). A lower but still significant correlation was observed between cRNA yield and both the number of detected genes and the average signal (Pearson = 0.44 and 0.36, respectively). These results confirmed that, at least for the Illumina platform and procedures, microarray data of technically good quality can be obtained from most FNA leftover samples.

We then proceeded by exploring in a quantitative manner if gene expression profiling highlights biologic features of the leftover samples rather than technical features associated with their preparation. We defined a set of numerical scores, each ranging from −3 to +3 and representing a biologic or technical variable, as illustrated in Table 3.

FNA leftovers were hierarchically clustered using Pearson correlation with complete linkage, based on the whole set of expressed genes (i.e., genes for which the GenomeStudio detection *P* value was 0 in at least two samples). The statistical robustness of the clusters was evaluated by a bootstrapping procedure [20]. As illustrated in Figure 4, FNA samples were clustered in three major branches, with reasonable consistency also in bootstrapped data (bootstrap probability of 77%, 97%, and 100%). The heat map below the clustering tree represents three categories of variables, respectively, from top

Table 3. Scores for Biologic and Technical Variables Used to Evaluate Sample Partitioning.

Score	−3	−2	−1	1	2	3
Variables of smears						
(1) Cellularity	low			Intermediate		high
(2) Nuclear grade						
(1) Stromal cells	no					yes
(2) Inflammatory cells						
Variables of histologic samples						
Mitoses/10 high-over field	0-9			10-19		20-50
ER or PgR (%)	0	1-19	20-39	40-59	60-79	80-100
Ki67 (%)	0-19			20-39		40-60
HER2 score	0			1+		3+
Technical variables						
(1) Average signal rank	1-2	3-4	5-6	7-8	9-10	11-12
(2) Detected genes rank						
Bioanalyzer RIN number	<5	5-6	—	6-7	7-8	>8
Spectrophotometer cRNA yield (ng/μl)	<150	150-299	300-449	450-599	600-749	>750

to bottom: 1) cytologic parameters of the FNA samples, 2) histopathologic parameters of the corresponding surgical samples, and 3) technical parameters associated to RNA expression profiling. It seems evident that biologic variables of FNA samples and derived surgical samples are more sharply partitioned by the expression-based clusters than by technical variables. In particular, the leftmost cluster is enriched in triple-negative, aggressive cancers, whereas the rightmost cluster is enriched in less aggressive, ER-positive tumors. The three cancers of special histologic type (endocrine, papillary, and lobular carcinomas, respectively, corresponding to samples F, M, and Q) were in the same central cluster, as expected by their biology. These results show that gene expression profiling partitions FNA leftover samples based on their biologic properties rather than on the quality/amount of RNA/cRNA obtained.

Classification of FNA Samples by Expression Profiling

We then investigated the possibility of using microarray analysis to define grade and ER, ERBB2/HER2 and Ki67 status directly on FNA leftovers. For this purpose, histologic grade and ER, ERBB2/HER2, and Ki67 immunohistochemical (IHC) data were available as a reference from surgical specimens of all the 23 profiled samples (Table W1).

To assess ER and ERBB2 status, we used single probes of the Illumina array. According to the ENSEMBL genome database (http://www.ensembl.org), these probes match equivalent Affymetrix probe sets previously found to correctly define ER and ERBB2 status of breast cancer samples [24] and further validated by us on large cohorts assembled from published Affymetrix data sets (Figures W1 and W2). As displayed in Figure 5, *A* and *B*, Illumina probes in our leftover data set were very good at partitioning samples: no single ER-negative sample had an ESR1 probe signal higher than the lowest ER-positive sample. Similarly, no ERBB2-positive sample (IHC score 3) had lower ERBB2 probe signal than the highest of the ERBB2-low/negative samples. In both cases, despite the limited sample size, the correlations between probe signals and ER or ERBB2 status were high

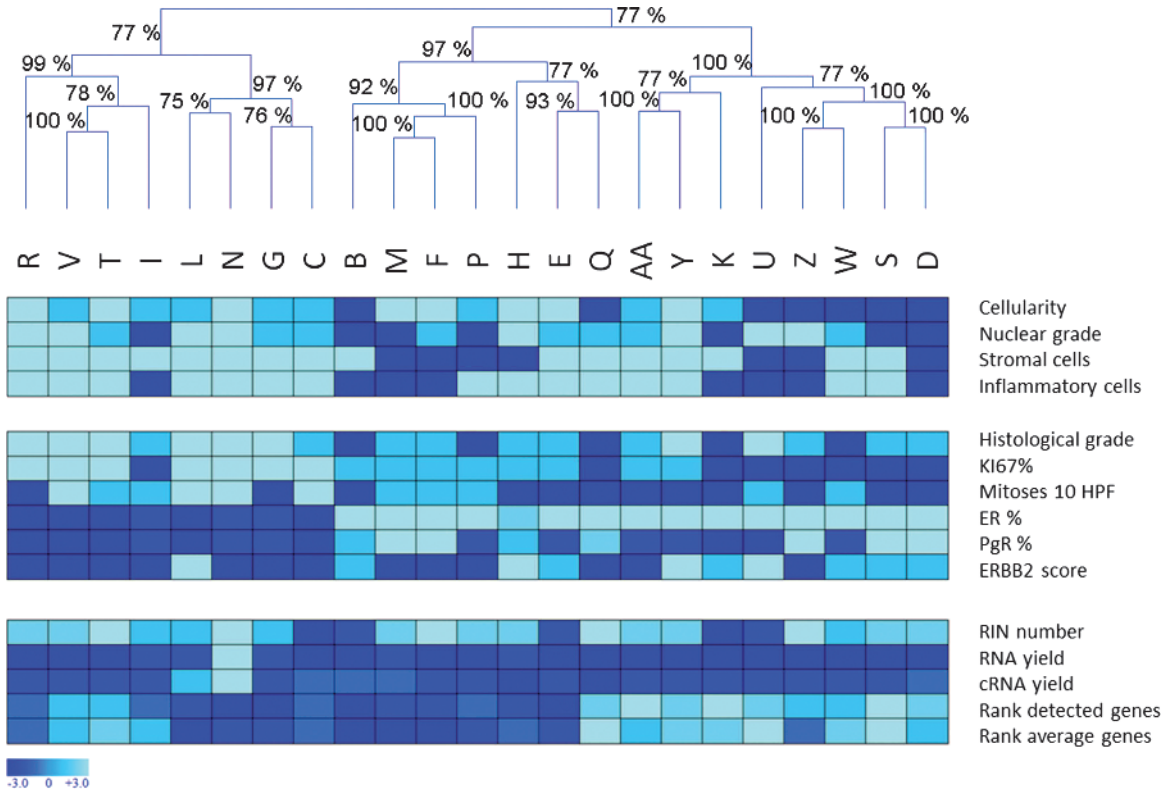

Figure 4. Hierarchical clustering of FNA leftover samples based on global gene expression. Each branch of the hierarchical tree is annotated with the probability value calculated by the pvclust tool on bootstrapped data. The heat map below the tree reports, for each sample, three categories of variables measured, respectively, on FNA samples (top, four rows), surgical specimens (middle, six rows), and RNA and microarrays (bottom, five rows).

enough to reach strong statistical significance and power (Pearson correlation = 0.98 and 0.89 for ER and ERBB2, respectively; $P < .0001$ and statistical power of 100% in both cases).

To evaluate tumor grade, we mapped on Illumina arrays the genes of the Genomic Grade signature originally developed by Sotiriou et al. [25] on Affymetrix arrays. We then used the original algorithm for genomic grade calculation on the FNA leftover samples: genomic and pathologic grade do not overlap completely but show a good correlation (Pearson correlation = 0.69, $P < .001$, statistical power = 98.67%), with grade 2 samples subdivided in genomic grade 1–like and genomic grade 3–like (Figure 5*C*). We then assessed the possibility of measuring the proliferative status of the tumor by analyzing correlation between Ki67 levels in the surgical specimens and average expression in the FNA leftovers of 53 proliferation genes extracted from two previous works defining breast cancer proliferation signatures [26,27]. Performances of such a proliferation signature were first assessed in an aggregated Affymetrix data set of 202 samples annotated with Ki67 status, with good results (Figure W3, *A* and *B*). On FNA leftovers, as shown in Figure 5*D*, the proliferation signature score was strongly correlated with Ki67 (Pearson correlation = 0.87, $P < .0001$, statistical power = 100%; Figure W3*C*). Interestingly, in no case did a sample with more than 30% Ki67-positive cells have a signature score lower than any sample with less than 30% positive cells.

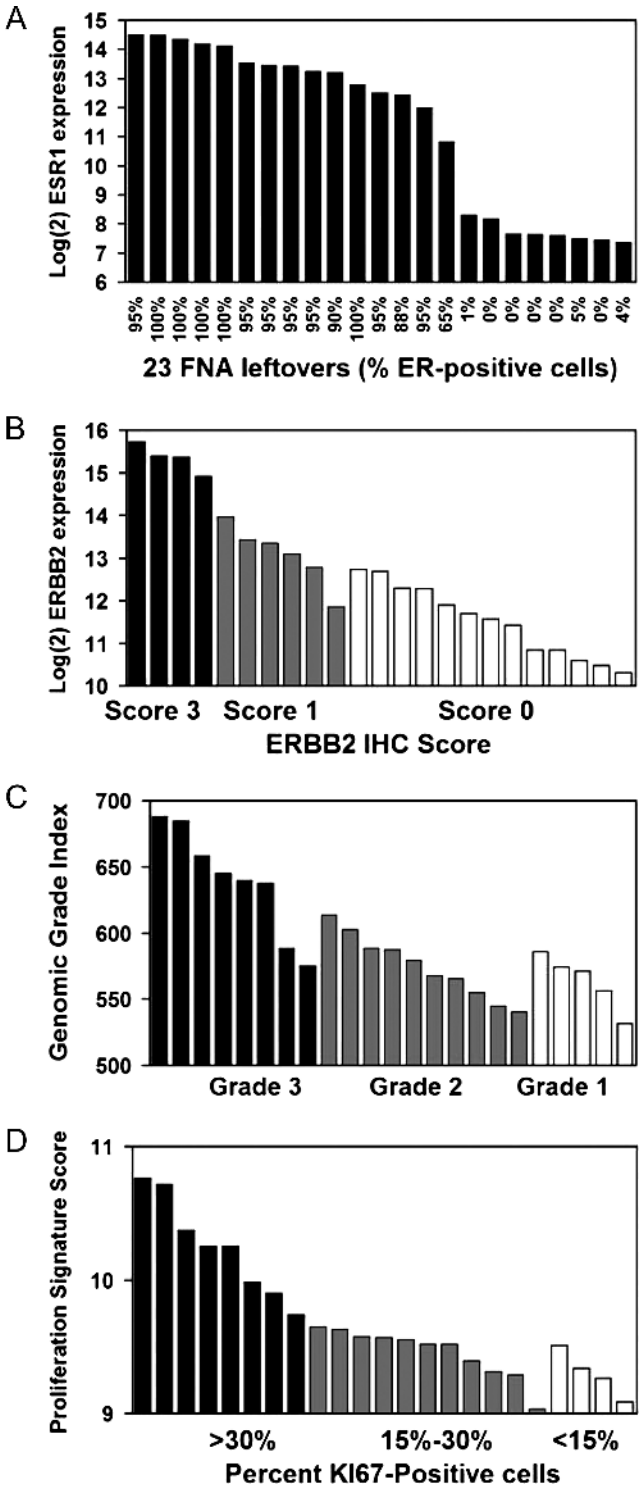

Discussion

In this study, we showed that the leftover, residual material from the smearing procedures of FNA samples, contains an important source of fresh cells, suitable for banking and appropriate for molecular analysis of small nonpalpable breast lesions. Our results demonstrate that RNA can be successfully extracted from the FNA leftovers. RNA was of good quality and quantity and allowed high-throughput molecular analysis procedures, such as gene expression profiling. Importantly, no technical factors were responsible for major biases in the analysis, as demonstrated by the fact that samples subjected to global gene expression analysis were clustered into biologically meaningful groups by their gene expression profile. Conversely, when technical variables were considered, a totally different clustering was observed with no clear correlation with the expression profile.

Most of the standardized molecular methods for measuring gene expression require either fresh or frozen tissues. Therefore, they pose major technical issues in timing, quantity, and quality of the material obtained from the sampling procedure. The timing issue has already been considered by Wong et al. [28] as a confounding factor in microarray data analysis because of the activation and increase of FOS hypoxia-related genes induced by ischemia of tissues taken from postoperative specimens compared with those obtained from *in vivo*

Figure 5. Use of microarray data to classify FNA leftover samples for ER status, HER2 status, grade, and proliferation. (A) Waterfall plot of microarray-based measurement of ESR1 gene expression on leftover samples, each annotated with the percent of ER-positive cells in IHC analysis of the respective surgical samples (*x* axis). (B) Waterfall plot of microarray-based measurement of ERBB2 gene expression on leftover samples, subdivided in HER2 score 3 (black bars), score 1 (gray bars), and Score 0 (white bars) based on IHC analysis of the respective surgical samples. (C) Waterfall plot of microarray-based measurement of the genomic grade on leftover samples, subdivided in histologic grade 3 (black bars), grade 2 (gray bars), and grade 1 (white bars) subgroups based on histologic grade assessments on the respective surgical samples. (D) Waterfall plot of microarray-based measurement of the 53-gene proliferation signature score on leftover samples, subdivided in three subgroups based on IHC analysis of the fraction of Ki67-positive cells in the respective surgical samples: more than 30% positive cells (black bars), 15% to 30% positive cells (gray bars), and less than 15% positive cells (white bars).

FNA sampling. Concerning the quantity of RNA, the method proposed here allows to obtain adequate samples even from nonpalpable, mammographically detected lesions, which are typically not suitable for tissue banking and therefore must be entirely formalin fixed and paraffin embedded for adequate histologic diagnosis. These results are consistent with previous findings [5–8,10,11,24] reporting feasibility and reliability of RNA extraction from cytologic samples of breast cancer. However, in those studies, additional passes were performed to retrieve material to be specifically used for molecular analysis [5–8,10,11]. This may constitute a bias particularly when dealing with small nonpalpable lesions because the adequacy of the sampling in correct targeting of the lesion was not taken into account. The issue of adequacy of the material subjected to molecular analyses is of paramount importance. In routine practice, a significant proportion of molecular tests performed on histologic tissue samples is not successful either because of underrepresentation of the cancer cells (focal tumor area in the sample with high amount of sclerosis) or because of incorrect sampling of the tumor area (no cancer cells in the sample). The onsite interpretation of the smears, currently performed in our protocol, guarantees a direct correlation with the imaging pattern and adequacy of both cytologic and molecular samples. In this study, we managed to obtain both diagnostic cells (from the smears) and tissue material dedicated to ancillary analyses (from the sample leftover) by exploiting a single FNA procedure in 92% of cases.

These results are even more appealing in light of a possible role of such molecular tests in guiding therapeutic decisions. A previous study by Gong et al. [24] has shown that the amount of ESR1 and HER2 mRNA as measured by the Affymetrix GeneChip reliably and reproducibly establish ER status and HER2 status, in different tissue samples including FNA. Here we show that, by using FNA leftovers, it is possible to accurately assess ER and HER2 expression by Illumina Gene Chip. Indeed, a good correlation with the IHC data assessed on surgical specimens derived from the same lesion was obtained. Although we are cautious because of the limited sample size, we observe that these results seem even better than those obtained with the respective Affymetrix probe sets in two cohorts of published data sets of 1605 samples for ER status and 655 samples for ERBB2 status, respectively (Figures W1 and W2). In addition, we successfully developed a multiprobe genomic signature for proliferation genes, finding very high correlation with the Ki67 status, and adapted to Illumina arrays the genomic grade index, with results that are fully compatible with those originally observed by Sotiriou et al. [25] on Affymetrix arrays. At present, these analyses are not requested by oncologist for routine management of breast cancer patients; however, they could be usefully applied to better define uncertain or borderline IHC results. Moreover, one should note that this analysis opens the door for the evaluation of biomarkers other than ER or HER2 that may be demonstrated as associated with sensitivity or resistance to different types of therapy.

In conclusion, our findings clearly show that cells residual from diagnostic FNA can be successfully used for RNA extraction and tumor banking of small nonpalpable breast cancer lesions. Most importantly, gene expression profiling of these residual cells reliably recapitulate the biology of the tumor specimen. Onsite adequacy assessment of FNA sampling ensures the correct targeting of the lesions both for cytologic and molecular analysis. This approach may be of particular interest if applied to FNA of abdominal or thoracic lesions, which are sampled under computed tomography and may need precise molecular test for target therapy.

Acknowledgments

The authors thank Elise Jackson for kindly reviewing the article and Roberta Porporato for technical support for Illumina microarray analysis.

References

[1] Marchiò C and Reis Filho JS (2008). Molecular diagnosis in breast cancer. *Diagn Mol Pathol* **14**, 202–213.

[2] Juhl H (2010). Preanalytical aspects: a neglected issue. *Scand J Clin Lab Invest Suppl* **242**, 63–65.

[3] Hicks DG, Kushner L, and McCarthy K (2011). Breast cancer predictive factor testing: the challenges and importance of standardizing tissue handling. *J Natl Cancer Inst Monogr* **2011**, 43–45.

[4] Lin DW, Coleman IM, Hawley S, Huang CY, Dumpit R, Gifford D, Kezele P, Hung H, Knudsen BS, Kristal AR, et al. (2006). Influence of surgical manipulation on prostate gene expression: implications for molecular correlates of treatment effects and disease prognosis. *J Clin Oncol* **24**, 3763–3770.

[5] Assersohn L, Gangi L, Zhao Y, Dowsett M, Simon R, Powles TJ, and Liu ET (2002). The feasibility of using fine needle aspiration from primary breast cancers for cDNA microarray analyses. *Clin Cancer Res* **8**, 794–801.

[6] Centeno BA, Enkemann SA, Coppola D, Huntsman S, Bloom G, and Yeatman TJ (2005). Classification of human tumors using gene expression profiles obtained after microarray analysis of fine-needle aspiration biopsy samples. *Cancer* **105**, 101–109.

[7] Lim EH, Aggarwal A, Agasthian T, Wong PS, Tan C, Sim E, Tan L, Goh PS, Wang SC, Khoo KL, et al. (2003). Feasibility of using low-volume tissue samples for gene expression profiling of advanced non–small cell lung cancers. *Clin Cancer Res* **9**, 5980–5987.

[8] Pusztai L, Ayers M, Stec J, Clark E, Hess K, Stivers D, Damokosh A, Sneige N, Buchholz TA, Esteva FJ, et al. (2003). Gene expression profiles obtained from fine-needle aspirations of breast cancer reliably identify routine prognostic markers and reveal large-scale molecular differences between estrogen-negative and estrogen-positive tumors. *Clin Cancer Res* **9**, 2406–2415.

[9] Sotiriou C, Khanna C, Jazaeri AA, Petersen D, and Liu ET (2002). Core biopsies can be used to distinguish differences in expression profiling by cDNA microarrays. *J Mol Diagn* **4**, 30–36.

[10] Sotiriou C, Powles TJ, Dowsett M, Jazaeri AA, Feldman AL, Assersohn L, Gadisetti C, Libutti SK, and Liu ET (2002). Gene expression profiles derived from fine needle aspiration correlate with response to systemic chemotherapy in breast cancer. *Breast Cancer Res* **4**, R3.

[11] Symmans WF, Ayers M, Clark EA, Stec J, Hess KR, Sneige N, Buchholz TA, Krishnamurthy S, Ibrahim NK, Buzdar AU, et al. (2003). Total RNA yield and microarray gene expression profiles from fine-needle aspiration biopsy and core-needle biopsy samples of breast carcinoma. *Cancer* **97**, 2960–2971.

[12] Uzan C, Andre F, Scott V, Laurent I, Azria E, Suciu V, Balleyguier C, Lacroix L, Delaloge S, and Vielh P (2009). Fine-needle aspiration for nucleic acid–based molecular analyses in breast cancer. *Cancer Cytopathol* **117**, 32–39.

[13] Andre F, Michiels S, Dessen P, Scott V, Suciu V, Uzan C, Lazar V, Lacroix L, Vassal G, Spielmann M, et al. (2009). Exonic expression profiling of breast cancer and benign lesions: a retrospective analysis. *Lancet Oncol* **10**, 381–390.

[14] Ladd AC, O'Sullivan-Mejia E, Lea T, Perry J, Dumur CI, Dragoescu E, Garrett CT, and Powers CN (2011). Preservation of fine-needle aspiration specimens for future use in RNA-based molecular testing. *Cancer Cytopathol* **119**, 102–110.

[15] Perry N, Broeders M, de Wolf C, Tornberg S, Holland R, and von Karsa L (2006). Chapter 6: FNAC Reporting Guidelines. In *European Guidelines for Quality Assurance in Breast Cancer Screening and Diagnosis* (4th ed). European Community, Luxembourg.

[16] Dabbs DJ and Silverman JF (1994). Prognostic factors from the fine-needle aspirate: breast carcinoma nuclear grade. *Diagn Cytopathol* **10**, 203–208.

[17] Don RH, Cox PT, Wainwright BJ, Baker K, and Mattick JS (1991). "Touchdown" PCR to circumvent spurious priming during gene amplification. *Nucleic Acids Res* **19**, 4008.

[18] Daniele L, Annaratone L, Allia E, Mariani S, Armando E, Bosco M, Macri L, Cassoni P, D'Armento G, Bussolati G, et al. (2009). Technical limits of comparison of step-sectioning, immunohistochemistry and RT-PCR on breast cancer sentinel nodes: a study on methacarn-fixed tissue. *J Cell Mol Med* **13**, 4042–4050.

[19] Fu L and Medico E (2007). FLAME, a novel fuzzy clustering method for the analysis of DNA microarray data. *BMC Bioinformatics* **8**, 3.

[20] Suzuki R and Shimodaira H (2006). Pvclust: an R package for assessing the uncertainty in hierarchical clustering. *Bioinformatics* **22**, 1540–1542.

[21] R: Development Core Team (2004). *R: A Language and Environment for Statistical Computing*. R Foundation for Statistical Computing, Vienna, Austria. Available at: http://www.r-project.org.

[22] Raman T, O'Connor TP, Hackett NR, Wang W, Harvey BG, Attiyeh MA, Dang DT, Teater M, and Crystal RG (2009). Quality control in microarray assessment of gene expression in human airway epithelium. *BMC Genomics* **10**, 493.

[23] Bussolati G, Annaratone L, Medico E, D'Armento G, and Sapino A (2011). Formalin fixation at low temperature better preserves nucleic acid integrity. *PLoS One* **6**, e21043.

[24] Gong Y, Yan K, Lin F, Anderson K, Sotiriou C, Andre F, Holmes FA, Valero V, Booser D, Pippen JE Jr, et al. (2007). Determination of oestrogen-receptor status and ERBB2 status of breast carcinoma: a gene-expression profiling study. *Lancet Oncol* **8**, 203–211.

[25] Sotiriou C, Wirapati P, Loi S, Harris A, Fox S, Smeds J, Nordgren H, Farmer P, Praz V, Haibe-Kains B, et al. (2006). Gene expression profiling in breast cancer: understanding the molecular basis of histologic grade to improve prognosis. *J Natl Cancer Inst* **98**, 262–272.

[26] Mira A, Isella C, Renzulli T, Cantarella D, Martelli ML, and Medico E (2009). The GAB2 signaling scaffold promotes anchorage independence and drives a transcriptional response associated with metastatic progression of breast cancer. *Oncogene* **28**, 4444–4455.

[27] Dai H, van't Veer L, Lamb J, He YD, Mao M, Fine BM, Bernards R, van de Vijver M, Deutsch P, Sachs A, et al. (2005). A cell proliferation signature is a marker of extremely poor outcome in a subpopulation of breast cancer patients. *Cancer Res* **65**, 4059–4066.

[28] Wong V, Wang DY, Warren K, Kulkarni S, Boerner S, Done SJ, and Leong WL (2008). The effects of timing of fine needle aspiration biopsies on gene expression profiles in breast cancers. *BMC Cancer* **8**, 277.

Supplementary Methods

In Silico *Analysis of* ESR1 *Expression in Breast Cancer*

For microarray-based assessment of ER status, we used expression of the *ESR1* gene measured by the Affymetrix probe set 205225_at, as previously suggested by Gong et al. [1]. An aggregated data set of 1605 ER status–annotated samples was generated by merging six published data sets [2–7].

Before plotting and receiver operating characteristic (ROC) curve analysis, the Log(2) signal for the probe set of choice was scaled based on the average signal of all probe sets included in a cross-mapping table generated by the Microarray Quality Control Consortium [8].

In Silico *Analysis of HER2 Expression in Breast Cancer*

For microarray-based assessment of HER2 status, we used the expression of the ERBB2 gene measured by the Affymetrix probe set 216836_s_at, as previously suggested by Gong et al. [1]. An aggregated data set of 655 samples annotated for HER2 status was generated by merging three published data sets [2,4,7]. Probe signal scaling was performed as described above for ESR1 analysis.

Genomic Grade Analysis

For microarray-based definition of the tumor grade in the FNA leftover samples, we applied the genomic grade signature published by Sotiriou et al. [5]. For our analysis, we mapped the genes of genomic grade signature, originally built on the Affymetrix platform, on the Illumina platform, using the above-mentioned MAQC table to obtain a set of genes reproducibly measured in different microarray platforms. The genomic grade index was then calculated for each of the 23 FNA leftovers as the difference between the sum of expression of genes associated to histologic grade 3 and the sum of expression of genes associated to histologic grade 1.

Definition and Validation of a Genomic Proliferation Signature

To build a microarray-based multigene classifier reflecting the proliferative status of the tumor, we built a "proliferation score" by averaging the Log(2) expression values of a set of 53 genes whose expression is positively correlated to cell proliferation, extracted from two published works [9,10]. The performance of this set of genes was evaluated by a ROC curve in a data set of 202 breast cancer samples [4] annotated for Ki67 status (area under the curve = 0.824; Figure W3*B*). The mean gene expression of the proliferation gene signature was then validated on the 23 FNA leftovers subdivided in three subgroups: high proliferation (more than 30% Ki67-positive cells), intermediate (15%-30% positive cells), and low proliferation (<15% positive cells), as shown in Figure 5*D*. An additional analysis of correlation with the fraction of Ki67-positive cells was performed using linear regression (Figure W3*C*). In the FNA leftovers data set, we also controlled the performance of the single probe measuring expression of the MKI67 gene, which showed worse correlation with the percentage of Ki67-positive cells (Pearson = 0.46 for the MKI67 gene and 0.76 for the 53-gene proliferation signature).

References

[1] Gong Y, Yan K, Lin F, Anderson K, Sotiriou C, Andre F, Holmes FA, Valero V, Booser D, Pippen JE Jr, et al. (2007). Determination of oestrogen-receptor status and ERBB2 status of breast carcinoma: a gene-expression profiling study. *Lancet Oncol* **8**, 203–211.

[2] Lee JK, Coutant C, Kim YC, Qi Y, Theodorescu D, Symmans WF, Baggerly K, Rouzier R, and Pusztai L (2010). Prospective comparison of clinical and genomic multivariate predictors of response to neoadjuvant chemotherapy in breast cancer. *Clin Cancer Res* **16**, 711–718.

[3] Miller LD, Smeds J, George J, Vega VB, Vergara L, Ploner A, Pawitan Y, Hall P, Klaar S, Liu ET, et al. (2005). An expression signature for p53 status in human breast cancer predicts mutation status, transcriptional effects, and patient survival. *Proc Natl Acad Sci USA* **102**, 13550–13555.

[4] Sabatier R, Finetti P, Cervera N, Lambaudie E, Esterni B, Mamessier E, Tallet A, Chabannon C, Extra JM, Jacquemier J, et al. (2011). A gene expression signature identifies two prognostic subgroups of basal breast cancer. *Breast Cancer Res Treat* **126**, 407–420.

[5] Sotiriou C, Wirapati P, Loi S, Harris A, Fox S, Smeds J, Nordgren H, Farmer P, Praz V, Haibe-Kains B, et al. (2006). Gene expression profiling in breast cancer: understanding the molecular basis of histologic grade to improve prognosis. *J Natl Cancer Inst* **98**, 262–272.

[6] Wang Y, Klijn JG, Zhang Y, Sieuwerts AM, Look MP, Yang F, Talantov D, Timmermans M, Meijer-van Gelder ME, Yu J, et al. (2005). Gene-expression profiles to predict distant metastasis of lymph-node–negative primary breast cancer. *Lancet* **365**, 671–679.

[7] Hess KR, Anderson K, Symmans WF, Valero V, Ibrahim N, Mejia JA, Booser D, Theriault RL, Buzdar AU, Dempsey PJ, et al. (2006). Pharmacogenomic predictor of sensitivity to preoperative chemotherapy with paclitaxel and fluorouracil, doxorubicin, and cyclophosphamide in breast cancer. *J Clin Oncol* **24**, 4236–4244.

[8] Shi L, Reid LH, Jones WD, Shippy R, Warrington JA, Baker SC, Collins PJ, de Longueville F, Kawasaki ES, Lee KY, et al. (2006). The MicroArray Quality Control (MAQC) project shows inter- and intraplatform reproducibility of gene expression measurements. *Nat Biotechnol* **24**, 1151–1161.

[9] Dai H, van't Veer L, Lamb J, He YD, Mao M, Fine BM, Bernards R, van de Vijver M, Deutsch P, Sachs A, et al. (2005). A cell proliferation signature is a marker of extremely poor outcome in a subpopulation of breast cancer patients. *Cancer Res* **65**, 4059–4066.

[10] Mira A, Isella C, Renzulli T, Cantarella D, Martelli ML, and Medico E (2009). The GAB2 signaling scaffold promotes anchorage independence and drives a transcriptional response associated with metastatic progression of breast cancer. *Oncogene* **28**, 4444–4455.

Table W1. ER, ERBB2/HER2, Ki67, and Histologic Grade Data from the 23 Matched Histologic Samples of Breast Cancers.

No.	Sample	ER (%)	HER2 (Score)	Ki67 (%)	Histologic Grade
2	B	90%	1+	28%	1
3	C	Negative	0	44%	2
4	D	95%	1+	6%	2
5	E	95%	1+	28%	2
6	F	100%	0	23%	2
7	G	4%	0	60%	3
8	H	65%	3+	34%	2
9	I	5%	0	17%	2
11	K	100%	1+	18%	1
12	L	Negative	3+	43%	3
13	M	100%	0	22%	2
14	N	1%	0	60%	3
16	P	95%	0	30%	1
17	Q	88%	0	11%	1
18	R	Negative	0	70%	3
19	S	100%	1+	14%	2
20	T	Negative	0	43%	3
21	U	95%	3+	16%	3
22	V	Negative	0	70%	3
23	W	95%	1+	19%	1
25	Y	95%	3+	25%	3
26	Z	100%	0	9%	2
27	AA	95%	0	21%	2

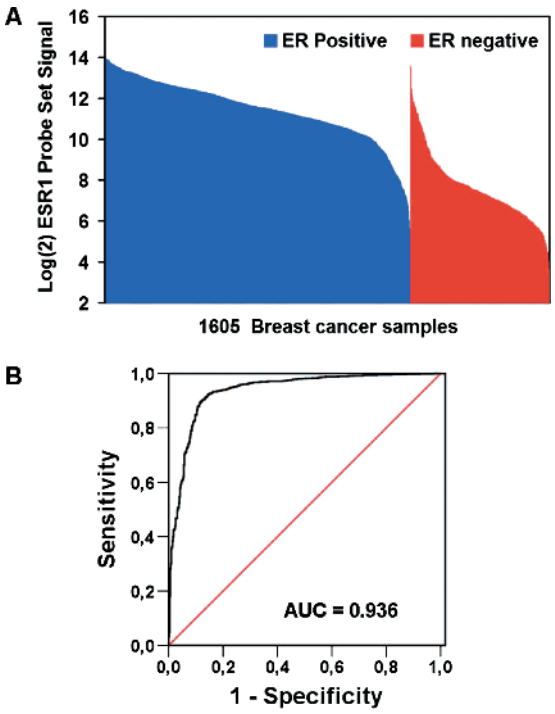

Figure W1. ESR1 expression measured by Affymetrix probe set in an aggregated data set of 1605 published samples. (A) Waterfall plot of ESR1 expression in samples annotated as ER-positive (blue) and ER-negative (red). (B) ROC curve analysis to evaluate sensitivity and specificity of the ESR1 Affymetrix probe set in detecting ER-positive *versus* ER-negative samples.

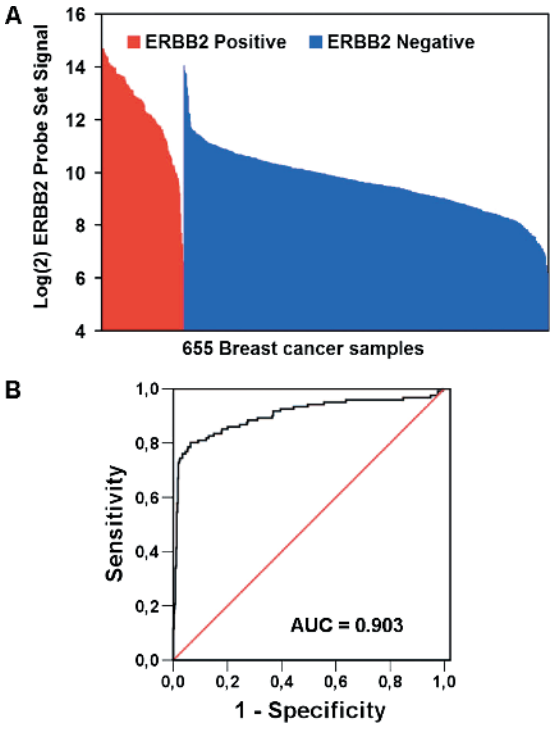

Figure W2. ERBB2 expression measured by Affymetrix probe set in an aggregated data set of 655 published samples. (A) Waterfall plot of ERBB2 expression in samples annotated as ERBB2-positive (red) and ERBB2-negative (blue). (B) ROC curve analysis to evaluate sensitivity and specificity of the ERBB2 Affymetrix probe set in detecting ERBB2-positive *versus* ERBB2-negative samples.

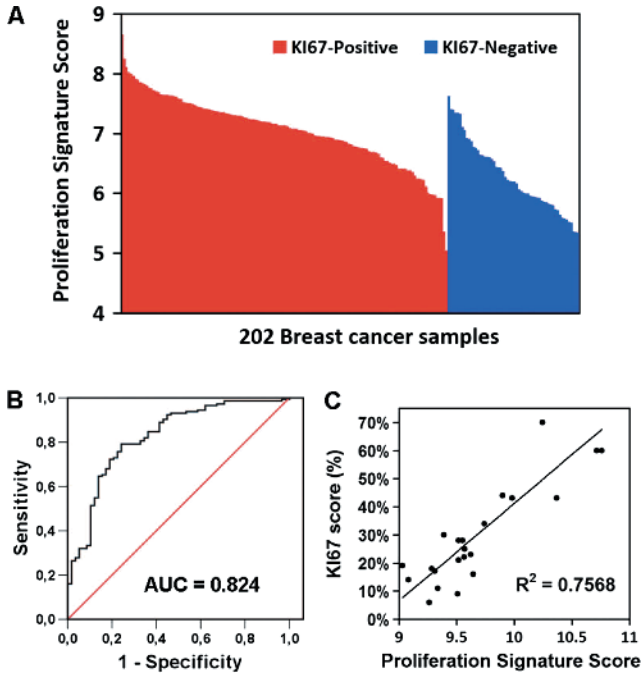

Figure W3. The 53-gene proliferation signature measured in an aggregated Affymetrix data set of 205 published samples and in 23 FNA leftovers samples. (A) Waterfall plot proliferation signature score in samples annotated as Ki67-positive (red) and Ki67-negative (blue). (B) ROC curve analysis to evaluate sensitivity and specificity of the proliferation signature score in detecting Ki67-positive *versus* -negative samples in the same data set. (C) Dot plot comparing, in FNA leftovers, the proliferation signature score (*x* axis) with the Ki67 score (percent positive cells, *y* axis) measured on the respective surgical specimens. The R^2 value of 0.7568 corresponds to a Pearson correlation of 0.87.